Processing and Application of Ceramics 16 [4] (2022) 328–334
https://doi.org/10.2298/PAC2204328C

Phase equilibria in the La_2O_3-Y_2O_3-Gd_2O_3 system at 1500 °C

Olga V. Chudinovych[1,2,*], Oleksandr I. Bykov[1], Anatoly V. Samelyuk[1]

[1]*Frantsevich Institute for Problems in Materials Science NAS of Ukraine, Kiev, Ukraine*
[2]*National Technical University of Ukraine "Igor Sikorsky Kyiv Polytechnic Institute", Kiev, Ukraine*

Received 10 June 2022; Received in revised form 16 September 2022; Accepted 10 October 2022

Abstract

The phase equilibria in the ternary La_2O_3-Y_2O_3-Gd_2O_3 system at 1500 °C were studied by X-ray diffraction, petrography and electron microscopy in the overall concentration range. The samples of different compositions have been prepared from nitrate acid solutions by evaporation, drying and calcination at 1100 and 1500 °C. The solid solutions based on various polymorphous forms of constituent phases and ordered phase of $LaYO_3$ were revealed in the system. The isothermal section of the phase diagram for the La_2O_3-Y_2O_3-Gd_2O_3 system has been developed. It was established that in the ternary La_2O_3-Y_2O_3-Gd_2O_3 system fields of solid solutions exist based on hexagonal (A) La_2O_3 phase, monoclinic (B) modifications of La_2O_3 and Gd_2O_3, cubic (C) modification of Y_2O_3, as well as perovskite-type structure of $LaYO_3$ (R) with rhombic distortions. The systematic study that covered the whole compositional range excluded the formation of new phases. The refined lattice parameters of the unit cell and the boundaries of the homogeneity fields for solid solutions were determined.

Keywords: *La_2O_3-Y_2O_3-Gd_2O_3 system, phase equilibria, isothermal section, lattice parameters*

I. Introduction

The phosphors based on lanthanides represent a perspective class of materials for photovoltaic devices [1–6]. The similarity between the ionic radii of RE^{3+} makes it possible to create different pairs of rare earth elements (for example, Yb-Er, Yb-Ho, Yb-Tm). Gadolinium oxide (Gd_2O_3) has excellent optical and chemical properties, low phonon energy (~600 cm^{-1}), high refractive index and heat resistance. All these features of Gd_2O_3 make it a promising material for use in the conversion of solar energy [1]. Interest in optical ceramics as laser and scintillation media is due to their high optical transparency, radiation resistance, high thermal conductivity, good thermomechanical properties, chemical resistance and thermal stability [1,7–11].

Data on the phase equilibria in the binary La_2O_3-Y_2O_3 system and its practical use are given in the literature [12–23]. This system is characterized by a peritectic transformation at 2310 °C for ~83 mol% Y_2O_3 and melting minimum at 2215 °C for 30 mol% Y_2O_3 [14,15,18]. Wide ranges of solid solutions based on different crystalline modifications of the components are formed in the system. Temperatures of polymorphic transformations in both yttrium doped La_2O_3 (X ⇆ H, H ⇆ A) and lanthanum doped yttria (H ⇆ C) decrease with doping content. The mutual solubility of the solid solutions increases with increasing temperature. In the A-form of La_2O_3 up to 30 mol% Y_2O_3 is dissolved at 1640 °C. The lattice parameters of the unit cell varies from a = 0.3935 nm, c = 0.6128 nm and c/a = 1.567 in the pure La_2O_3 to a = 0.3865 nm, c = 0.6072 nm and c/a = 1.571 in the sample containing 30 mol% Y_2O_3. The refractive indexes in the same concentration range are reduced from n_g = 2.10, n_p = 2.08 to 2.06 > n_g > 2.05, 2.04 > n_p > 2.03.

The solubility of La_2O_3 in the C-Y_2O_3 in the temperature range 1350–1900 °C varies insignificantly around 15 mol% La_2O_3. An intermediate compound $LaYO_3$ (R), crystallizing in the perovskite-type structure with rhombic distortion is formed in the system. The lattice parameters of the unit cell of the ordered phase $LaYO_3$ are equal to: a = 0.5883 nm, b = 0.6093 nm and c = 0.8501 nm. Crystal and optical characteristics of the $LaYO_3$ are: colourless crystals, anisotropic, biaxial, negative, $2V \approx 90°$ (angle between the axes), n_p = 1.98; n_g = 2.03. The R phase exists in the narrow homogeneity range (48–53 mol% Y_2O_3 at 1350 °C). This lattice parameters are reduced from a = 0.5895 nm, b = 0.6102 nm and c = 0.8510 nm at 48 mol% Y_2O_3 to

*Corresponding author: tel: +38 500860379
e-mail: *chudinovych_olia@ukr.net*

a = 0.5878 nm, b = 0.6085 nm and c = 0.8497 nm at 53 mol% Y_2O_3. The maximum temperature of the ordered phase $LaYO_3$ existence is about 1585 °C in the binary system. Above this temperature, a disordered phase of variable composition is formed and indicates the B-type rare-earth oxides of monoclinic structure. It undergoes at least two transformations by eutectoid and peritectoid reactions:

$$\langle B\rangle \leftrightarrows \langle LaYO_3\rangle + \langle C\rangle \text{ (55 mol\% } Y_2O_3, 1570\ ^\circ C) \quad (1)$$

$$\langle B\rangle + \langle C\rangle \leftrightarrows \langle H\rangle \text{ (71 mol\% } Y_2O_3, 1900\ ^\circ C) \quad (2)$$

On the curves separating the field of solid solutions based on the H-form of rare-earth oxides from the fields of solid solutions based on the A-, B- and C-modifications of rare-earth oxides, there are eutectoid point coordinated at 45 mol% Y_2O_3 and 1730 °C and peritectoid point at 71 mol% Y_2O_3 and 1900 °C [14,18].

In the Gd_2O_3-Y_2O_3 system, solid solutions of different lengths are formed based on B-, A-, H- and X-polymorphic forms of Gd_2O_3 together with C- and H-forms of Y_2O_3 [24]. The length of the region of solid solutions based on X-form in this system is much smaller than in Sm_2O_3-Y_2O_3 [24]. On the curve that separates the fields of solid solutions based on X- and H-forms from the two-phase regions of the solid solutions based on A-, B-, C-, H- and X-forms, there is an eutectoid point with coordinates 2190 °C, 22 mol% Y_2O_3 and peritectoid with coordinates 2240 °C, 65 mol% Y_2O_3. The range of the B-phase expands with increasing temperature. The limits of solid solutions based on B-Gd_2O_3 at 1300, 1700 and 1900 °C are 5, 25 and 36 mol% Y_2O_3, respectively.

The solubility of Gd_2O_3 in the C-form of yttrium oxide also depends significantly on temperature and is 90, 67 and 57 mol% at 1300, 1700 and 1900 °C, respectively. The lattice parameters of the unit cell increase from a = 1.0604 nm and V = 1.193 nm^3 for Y_2O_3 to a = 1.0772 nm and V = 1.250 nm^3 (at 1300 °C), a = 1.0723 nm and V = 1.233 nm^3 (at 1700 °C), a = 1.0712 nm and V = 1.229 nm^3 (at 1900 °C) [24].

Data on the phase equilibria in the binary La_2O_3-Gd_2O_3 system and its practical use are given in the literature [16,25–30]. Three types of continuous solid solutions based on hexagonal (A and H) and cubic (X) modifications of REE oxides form in the La_2O_3-Gd_2O_3 system. The region of homogeneity of solid solutions based on monoclinic (B) modification of Gd_2O_3 is limited. The maximum temperature of the existence of a solid solution based on B-Gd_2O_3 is 2080 °C, which corresponds to the phase transformation temperature of pure Gd_2O_3. The solubility of La_2O_3 in B-Gd_2O_3 is 10 mol% at 2020 °C, 20 mol% at 1900 °C and 50 mol% at 1580 °C [26]. The phase transition A ⇆ H in the La_2O_3-Gd_2O_3 system was recorded only by thermal analysis in the presence of an exothermic effect on the cooling curves. The minimum of the system is near the composition of 60 mol% La_2O_3 and ~2300 °C.

Phase equilibria in binary systems based on oxides of rare earth elements have been studied in full [13–31]. Information on phase equilibria in the ternary La_2O_3-Y_2O_3-Gd_2O_3 system is limited and requires further research. The purpose of this work is to study the interaction of lanthanum, yttrium and gadolinium oxides at 1500 °C in the entire concentration range and to construct the corresponding isothermal section.

II. Experimental

Lanthanum oxide (La_2O_3, LaO-1 grade), yttrium oxide (Y_2O_3, Merck Corp.), gadolinium oxide, (Gd_2O_3, Merck Corp.) with purity of 99.99% and analytical grade nitric acid were used as the starting materials. Powders of lanthania, yttria and gadolinia were preliminary dried at 200 °C for 20 h followed by dissolving in hot diluted nitric acid (1:1). Samples were prepared in concentration steps 1–5 mol% from nitrate solutions with their subsequent evaporation and decomposition at 800 °C for 2 h. The prepared powders were pressed at 10 MPa into pellets of 5 mm in diameter and 4 mm in height. To study phase relationships at 1500 °C the as-prepared samples were thermally treated in two stages: at 1100 °C (for 168 h in air) and then at 1500 °C (for 60 h in air) in the furnaces with heating elements based on Fecral (H23U5T) and Superkanthal ($MoSi_2$), respectively. The heating rate was 3.5 °C/min. Annealing of the samples was continuous and cooling was carried out within the furnace.

The samples were studied by XRD (DRON-3, Burevestnik, Leningrad), petrography (MIN-8, optical microscope) and electron microprobe X-ray (SUPERPROBE-733, JEOL, Japan, Palo Alto, CA) analyses.

The X-ray analysis of the samples was performed by powder method using DRON-3 at room temperature (CuKα radiation) with step size of 0.05–0.1° in 2θ

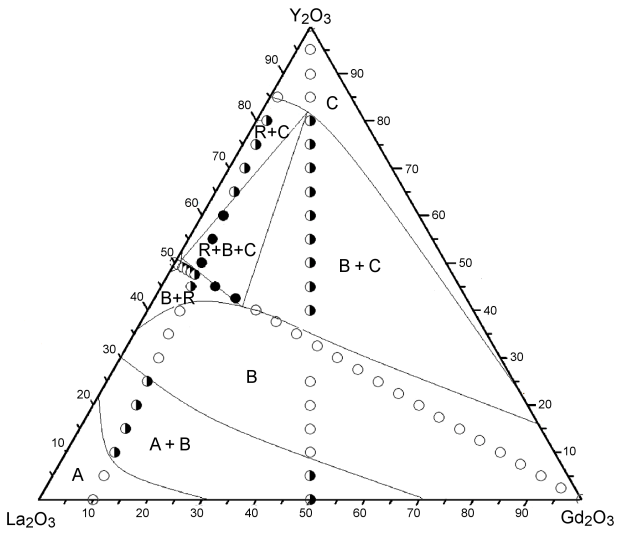

Figure 1. Isothermal sections at 1500 °C for the La_2O_3-Y_2O_3-Gd_2O_3 system (○ - single-phase samples, ◑ - two-phase samples, ● - three-phase samples)

range 15–90°. Lattice parameters were refined by least squares fitting using the LATTIC program [32]. The accuracy in the lattice parameter of cubic phases was within 0.0002 nm. Phase composition has been determined in accordance to the International powder standards (JSPDS International Center for Diffraction Data 1999).

The composition of the samples was monitored by spectral and chemical analysis selectively. The petrographic studies of annealed samples were carried in polarized light. The optical characteristics were specified in polarizing microscope MIN-8 with the aid of highly refractive immersion liquids.

Microstructures were examined on polished sections and rough fractured surfaces of annealed samples in backscattered electron (COMPO) and secondary electron (SE) modes by electron-probe X-ray microanalysis (EPXMA).

III. Results and discussion

Compositions of the investigated samples fall into three sections: Y_2O_3-(50 mol% La_2O_3 - 50 mol% Gd_2O_3), Gd_2O_3-(50 mol% La_2O_3 - 50 mol% Y_2O_3), Y_2O_3-(90 mol% La_2O_3 - 10 mol% Gd_2O_3). The obtained samples are labelled as follows: xY_2O_3-yLa_2O_3-zGd_2O_3, where x, y and z are mol% of Y_2O_3, La_2O_3 and Gd_2O_3, respectively. Chemical and phase compositions of the samples annealed at 1500 °C and parameters of the phases that are in equilibrium at this temperature are summarized in Electronic Supporting Information[§] Tables S1–S3. These results were used to construct the isothermal section of the La_2O_3-Y_2O_3-Gd_2O_3 phase diagram at 1500 °C (Fig. 1).

It is established that at 1500 °C in the La_2O_3-Y_2O_3-Gd_2O_3 system solution fields are formed based on cubic (C) modification of Y_2O_3, hexagonal (A) modification of La_2O_3 and monoclinic (B) modifications of La_2O_3 and Gd_2O_3, as well as ordered phase structure perovskite-type $LaYO_3$ (R). The boundaries of the homogeneity ranges for the phases formed in the system were determined according to the data provided in Tables S1–S3 (Electronic Supporting Information) and composition dependences for lattice parameters of the solid solutions.

In the region with a high content of Y_2O_3, single phase solid solutions are formed based on the cubic modification of yttrium oxide. The homogeneity range of the C-phase extends in compliance with its solubility limits in the boundary binary La_2O_3-Y_2O_3 (85–100 mol% Y_2O_3) and Y_2O_3-Gd_2O_3 (23–100 mol% Y_2O_3) systems. The field of solid solutions based on C- Y_2O_3 extends from 83 to 100 mol% Y_2O_3 at section Y_2O_3-(50 mol% La_2O_3 - 50 mol% Gd_2O_3) (Fig. 2). Microstructures and diffractograms of the solid solutions based on C- Y_2O_3 are presented in Figs. 3c,d and 4a, respectively.

In the ternary system La_2O_3-Y_2O_3-Gd_2O_3 at 1500 °C, the ordered phase of perovskite type with

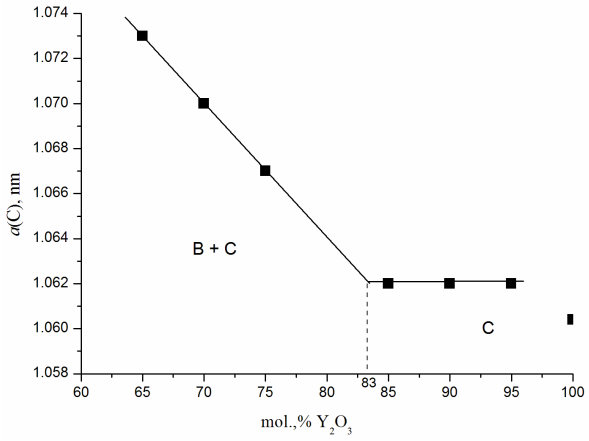

Figure 2. Concentration dependence for lattice parameter *a* of the solid solutions based on C-Y_2O_3 at section Y_2O_3-(50 mol% La_2O_3 - 50 mol% Gd_2O_3) annealed at 1500 °C

rhombic distortion has been revealed. The maximum solubility of gadolinium oxide in the R-phase is ~1.5 mol% along section Gd_2O_3-(50 mol% La_2O_3 - 50 mol% Y_2O_3). The lattice parameters of the R-phase unit cell vary from a = 0.5868 nm, b = 0.6084 nm, c = 0.8474 nm in the single-phase sample 1 Gd_2O_3-49.5 La_2O_3-49.5 Y_2O_3 to a = 0.5715 nm, b = 0.6117 nm, c = 0.8563 nm in the two-phase (R + B) sample 2 Gd_2O_3-49 La_2O_3-49 Y_2O_3. X-ray diffraction patterns of the samples that characterize the phase field with R-phase in the La_2O_3-Y_2O_3-Gd_2O_3 system at 1500 °C are presented in Figs. 4b,g. The formation of the R-phase was also observed in some other systems: La_2O_3-Y_2O_3-Nd_2O_3 [33], La_2O_3-Y_2O_3-Sm_2O_3 [34], La_2O_3-Y_2O_3-Er_2O_3 [35] and La_2O_3-Y_2O_3-Yb_2O_3 [36] at 1500 °C.

In the investigated La_2O_3-Y_2O_3-Gd_2O_3 system at 1500 °C three-phase region (B + C + R) was also formed. The sample 60 Y_2O_3-36 La_2O_3-4 Gd_2O_3 was characterized by three components that differ in contrast and morphology (Fig. 3i). The matrix is a light phase $LaYO_3$ (R), which shows fine-grained point inclusions of the cubic modification of C-Y_2O_3. The grey phase, enriched with lanthanum, is a monoclinic B-form of La_2O_3.

The microstructures of the samples that characterize the two-phase regions (B + C), (R + C), and (R + B) are presented in Fig. 3. The two structural components are clearly distinguished by contrast.

The system forms an infinite series of single phase solid solutions based on the monoclinic modification of B-La_2O_3 (Gd_2O_3). The homogeneity range of the B-phase passes under its solubility limits in the boundary binary La_2O_3-Y_2O_3, Gd_2O_3-Y_2O_3 and La_2O_3-Gd_2O_3 systems. The homogeneity range of the B-phase at section Y_2O_3-(50 mol% La_2O_3 - 50 mol% Gd_2O_3) extends from 9 to 33 mol% Y_2O_3 at 1500 °C (Fig. 5). X-ray diffraction patterns and microstructures of solid solutions based on the B-phase are presented in Figs. 4d and 3a,b, respectively. The formation of a continuous series

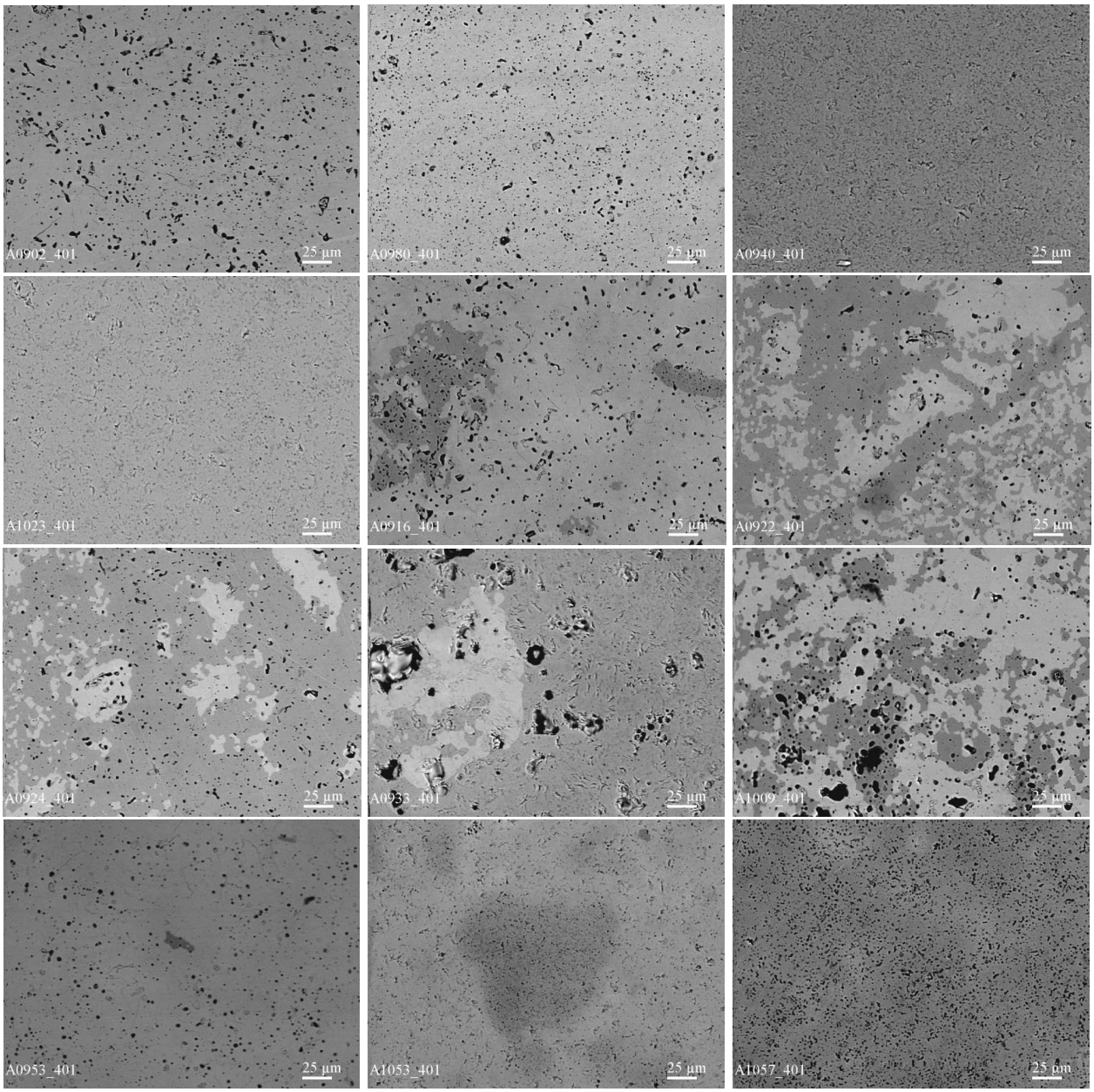

Figure 3. SEM micrographs of the La_2O_3-Y_2O_3-Gd_2O_3 samples heat-treated at 1500 °C: a) 10 Y_2O_3-45 La_2O_3-45 Gd_2O_3 <B>, b) 15 Y_2O_3-15 La_2O_3-70 Gd_2O_3 <B>, c) 95 Y_2O_3-2.5 La_2O_3-2.5 Gd_2O_3 <C>, d) 95 Y_2O_3-4.5 La_2O_3-0.5 Gd_2O_3 <C>, e) 40 Y_2O_3-30 La_2O_3-30 Gd_2O_3 <C>+<B>, f) 55 Y_2O_3-22.5 La_2O_3-22.5 Gd_2O_3 <C>+<B>, g) 60 Y_2O_3-20 La_2O_3-20 Gd_2O_3 <C>+<B>, h) 80 Y_2O_3-10 La_2O_3-10 Gd_2O_3 <C>+<B>, i) 60 Y_2O_3-36 La_2O_3-4 Gd_2O_3 <C>+<B>+R, j) 48 Y_2O_3-48 La_2O_3-4 Gd_2O_3 <B>+R, k) 70 Y_2O_3-27 La_2O_3-3 Gd_2O_3 <C>+R and l) 80 Y_2O_3-18 La_2O_3-2 Gd_2O_3 <C>+R

of solid solutions based on the B-phase means that the La^{3+} ions are replaced by Gd^{3+} in the crystal lattice and vice versa. Yttrium oxide stabilizes the complete mutual solubility of lanthanum and gadolinium oxides ($r_{La^{3+}}$ = 0.114 nm, $r_{Gd^{3+}}$ = 0.097 nm, $r_{Y^{3+}}$ = 0.092 nm). As the concentration of yttrium oxide increases, the parameters of the B-phase unit cell decrease, and the lattice of solid solutions based on the B-form of REE oxides becomes more densely packed.

In the region with a high content of La_2O_3, single phase solid solutions are formed based on the hexagonal modification of lanthanum oxide. Note that the oxide of lanthanum in air is subjected to hydration and thus, instead of hexagonal phase La_2O_3 in samples at 1500 °C we find the formation of hexagonal hydroxide of $La(OH)_3$. For XRD data in these samples, instead of the hexagonal modification of La_2O_3, the hexagonal modification of A- $La(OH)_3$ is provided (Figs. 4c,e). The lattice parameters vary from a = 0.6490 nm, c = 0.3884 nm, c/a = 0.5985 for the solid solution 90 La_2O_3-0 Y_2O_3-10 Gd_2O_3 to a = 0.6462 nm, c = 0.3859 nm, c/a = 0.5972 for the 76.5 La_2O_3-15 Y_2O_3-8.5 Gd_2O_3 two-phase sample (A + B).

The homogeneity range of the A-phase is not extensive and is concave in the direction of decreasing yttrium oxide content and passes under its solubility

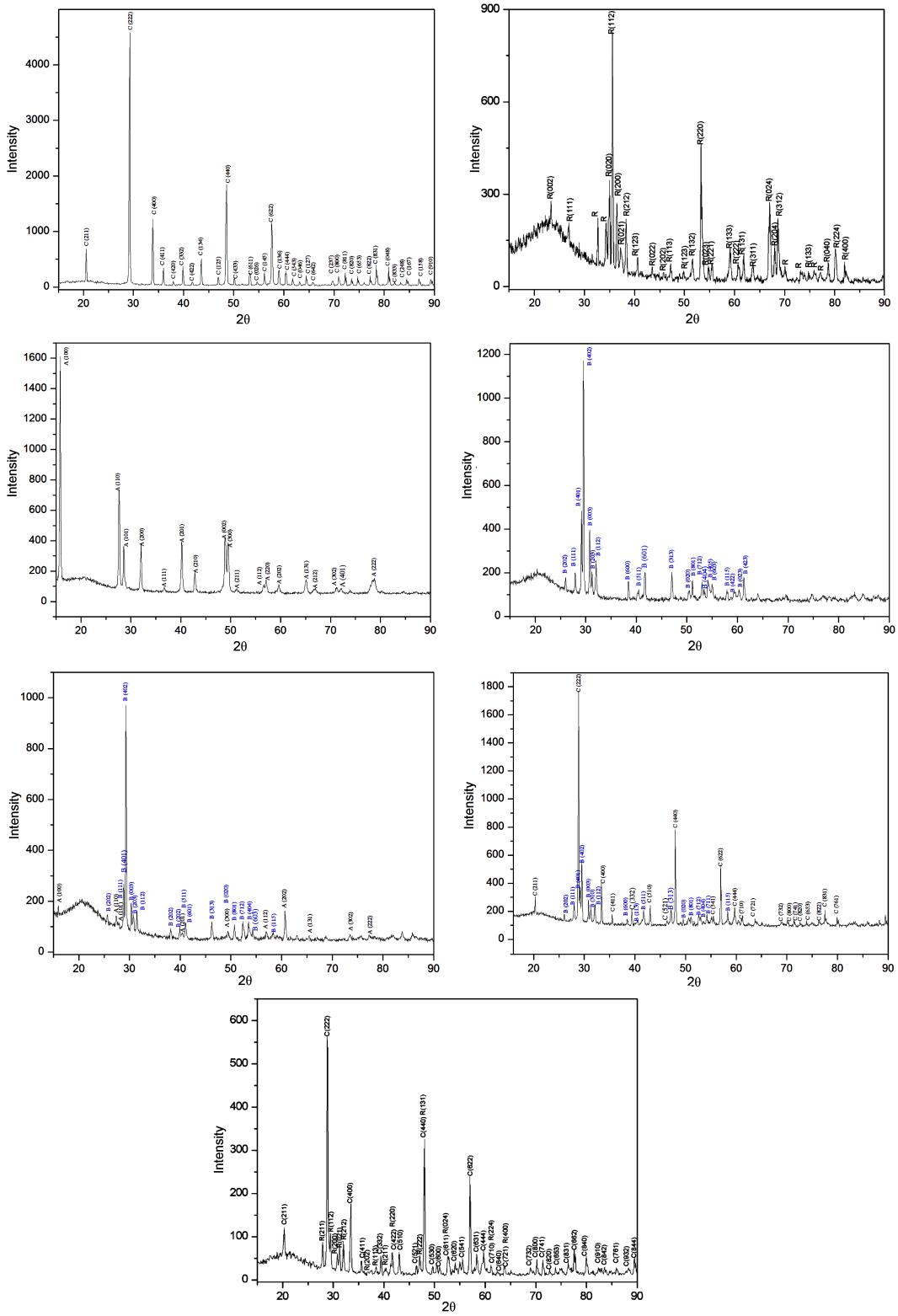

Figure 4. XRD patterns of the La_2O_3-Y_2O_3-Gd_2O_3 samples heat-treated at 1500 °C: a) 90 Y_2O_3-5 La_2O_3-5 Gd_2O_3 (C), b) 49.5 Y_2O_3-49.5 La_2O_3-1 Gd_2O_3, (R, $LaYO_3$), c) 5 Y_2O_3-85.5 La_2O_3-9.5 Gd_2O_3, (A*), d) 10 Y_2O_3-10 La_2O_3-80 Gd_2O_3 (B), e) 10 Y_2O_3-81 La_2O_3-9 Gd_2O_3, (A* + B), f) 60 Y_2O_3-20 La_2O_3-20 Gd_2O_3, (C + B) and g) 75 Y_2O_3-22.5 La_2O_3-2.5 Gd_2O_3, (C + R)

limits in the boundary binary La_2O_3-Y_2O_3 and La_2O_3-Gd_2O_3 systems. The solubility of yttrium oxide in the A phase is 9 mol% along section Y_2O_3-(90 mol% La_2O_3 - 10 mol% Gd_2O_3) as can be seen from Fig. 6. The formation of the A-phase was observed in some systems, such as: La_2O_3-Y_2O_3-Nd_2O_3 [33] and La_2O_3-Y_2O_3-Sm_2O_3 [34] at 1500 °C. For comparison, in the system La_2O_3-Y_2O_3-Nd_2O_3 we observe the formation of a continuous series of solid solutions based on the A-phase, while in the system La_2O_3-Y_2O_3-Gd_2O_3 a limited region of

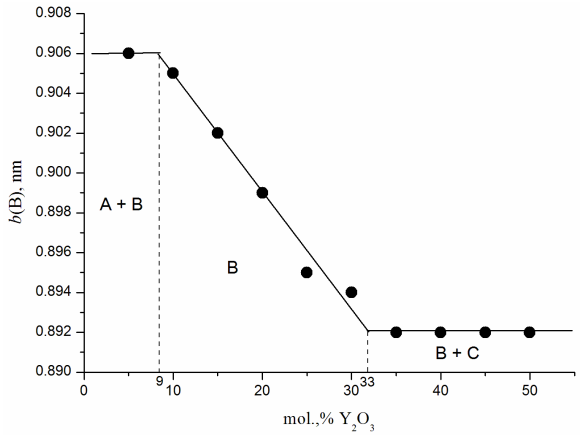

Figure 5. Concentration dependence of lattice parameter *b* of the solid solutions based on B-Gd_2O_3 at section Y_2O_3-(50 mol% La_2O_3 - 50 mol% Gd_2O_3) of the La_2O_3-Y_2O_3-Gd_2O_3 system after annealing at 1500 °C

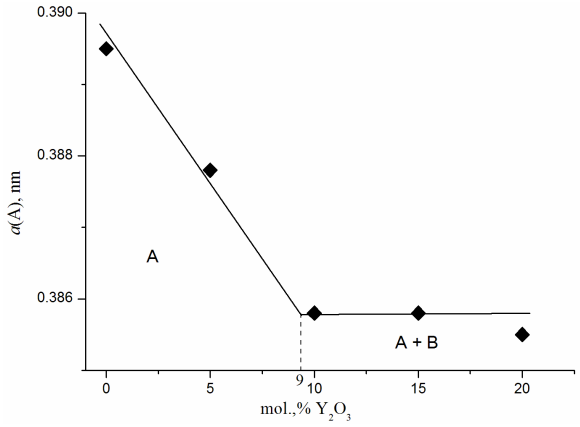

Figure 6. Concentration dependence of lattice parameter *a* of the solid solutions based on A-$La(OH)_3$ at section Y_2O_3-(50 mol% La_2O_3 - 50 mol% Gd_2O_3) of the La_2O_3-Y_2O_3-Gd_2O_3 system after annealing at 1500 °C

these solid solutions is formed. In the La_2O_3-Y_2O_3-Sm_2O_3 system at 1500 °C, the solubility of yttrium oxide in the A-phase is also ~9 mol% along section Y_2O_3-(90 mol% La_2O_3 - 10 mol% Sm_2O_3).

To determine the location of phase boundaries, results of the petrographic analysis were used along with the XRD data on the phase composition of the samples. The petrographic analysis confirmed X-ray diffraction data for the two-phase (A + B) sample 10 Y_2O_3-81 La_2O_3-9 Gd_2O_3. This sample clearly shows two structural components: A-$La(OH)_3$, which forms the basis, and the anisotropic phase B-Gd_2O_3 in the form of translucent particles with high relief and refractive index, which is present in significantly smaller quantities. At the same time, the sample 20 Y_2O_3-40 La_2O_3-40 Gd_2O_3 contains only one anisotropic B-phase with high interference colours and refractive index.

IV. Conclusions

Phase equilibria were studied in the La_2O_3-Y_2O_3-Gd_2O_3 system at 1500 °C. It has been established that solid state interactions between three oxides resulted in the formation of extended fields of solid solutions based on various crystal modifications of the initial components of rare-earth oxides, as well as the ordered phase of perovskite type $LaYO_3$ (R). The isothermal section of the system is characterized by three single-phase (A-La_2O_3, B-La_2O_3 (Gd_2O_3), C-Y_2O_3), three-phase (B + C + R) and two-phase (A + B, B + R, C + R, B + C) regions.

§ Supplementary data can be downloaded using following link: https://bit.ly/3VwupX6

References

1. A. Zatsepin, Y. Kuznetsova, L. Spallino, V. Pustovarov, V. Rychkov, "Photosensitive defects in Gd_2O_3 – Advanced material for solar energy conversion", *Energy Procedia*, **102** (2016) 144–151.
2. S.F. Wang, J. Zhang, D.W. Luo, F. Gu, D.Y .Tang, Z.L .Dong, G.E.B. Tan, W.X. Que, T.S. Zhang, S. Li, L.B. Kong, "Transparent ceramics: Processing, materials and applications", *Prog. Solid State Chem.*, **41** (2013) 20–54.
3. J. Sanghera, S. Bayya, G. Villalobos, W. Kim, J. Frantz, B. Shaw, B. Sadowski, R. Miklos, C. Baker, M. Hunt, I. Aggarwal, F. Kung, "Transparent ceramics for high-energy laser systems", *Opt. Mater.*, **33** (2011) 511–518.
4. B.S. Chen, W. Yiquan, "New opportunities for transparent ceramics", *Am. Ceram. Soc. Bull.*, **2** (2013) 32–37.
5. J. Akiyama, Y. Sato, T. Taira, "Laser ceramics with rare-earth-doped anisotropic materials", *Optics Lett.*, **35** (2010) 3598–3600.
6. T. Taira, "Domain-controlled laser ceramics toward Giant Micro-photonics", *Opt. Mater. Express*, **1** (2011) 1040–1050.
7. L. Zehua, S. Li, Y. Huang, L. Wang, Y. Yao, T. Long, X. Yao, X. Liu, Z. Huang, "Composite ceramic with high saturation input powder in solid-state laser lighting: Microstructure, properties, and luminous emittances", *Ceram. Int.*, **44** (2018) 20232–20238.
8. I.K. Jones, Z.M. Seeley, N. Cherepy, E.B. Duoss, S. Payne, "Direct ink write fabrication of transparent ceramic gain media", *Opt. Mater.*, **75** (2018) 19–25.
9. L. Liu, Q. Zhu, Q. Zhu, B. Jiang, M. Feng, L. Zhang. "Fabrication of fine-grained undoped Y_2O_3 transparent ceramic using nitrate pyrogenation synthesized nanopowders", *Ceram. Int.*, **45** (2019) 5339–5345.
10. Y. Zhang, I.-H. Jung, "Critical evaluation of thermodynamic properties of rare earth sesquioxides (RE = La, Ce, Pr, Nd, Pm, Sm, Eu, Gd, Tb, Dy, Ho, Er, Tm, Yb, Lu, Sc and Y)", *Calphad*, **58** (2017) 169–203.
11. A. Navrotsky, W. Lee, A. Mielewczyk-Gryn, S.V. Ushakova, A. Anderkoc, H. Wud, R.C. Rimand. Thermodynamics of solid phases containing rare earth oxides, *J. Chem. Thermodynam.*, **88** (2015) 1–56.
12. I. Hiroyuki, I. Naboru, T. Hirosi, T. Katsumori, S. Syundzyu, S. Yosio, "Materials for sealing between ceramic parts, and metal", *Patent No. 58-41766*, Japan, 1981.
13. M. Yoshimura, X.Z. Rong, "Various solid solutions in the systems Y_2O_3-R_2O_3 (R = La, Nd, and Sm) at high temperature", *J. Mater. Sci. Lett.*, **16** (1997) 1961–1963.
14. E.R. Andrievskaya, *Phase Equilibria in the Systems of Hafnia, Yttria with Rare-Earth Oxides* (in Russian), Scientific Book Project, Naukova Dumka, Kiev, 2010, pp. 480.

15. E.R. Andrievskaya, "Phase equilibria in the refractory oxide systems of zirconia, hafnia and yttria with rare-earth oxides", *J. Eur. Ceram. Soc*., **28** (2008) 2363–2388.
16. J. Coutures, A. Rouanet, R. Verges M. Foex, "Etude a haute temperature des systems formes par le sesquioxyde de lanthane et les sesquioxydes de lanthanides. I. Diagrammes de phases (1400 °C < T < T liquide)", *J. Solid State Chem.*, **17** (1976) 172–182.
17. J. Coutures, F. Sibieude, M. Foex, "Etude a haute température des systèmes formés par les sesquioxydes de lanthane avec les sesquioxydes de lanthanides. II. Influence de la trempe sur la nature des phases obtenues à la température ambiante", *J. Solid State Chem*., **17** (1976) 377–384.
18. L.M. Lopato, B.S. Nigmanov, A.V. Shevchenko, Z.A. Zaitseva, "Reaction of lanthanum oxide with yttrium oxide" (in Russian), *Izv. Akad. Nauk. SSSR Neorg. Mater.*, **22** (1986) 771–774.
19. V. Berndt, D. Maier, C. Keller, "New $A^{III}B^{III}O_3$ interlanthanide perovskite compounds", *J. Solid State Chem*., **13** (1975) 131–135.
20. M. Mizuno, A. Rouanet, T. Yamada, T. Noguchi, "Phase diagram of the system La_2O_3-Y_2O_3 at high temperatures", *J. Ceram. Soc. Jpn*., **84** (1976) 342–347.
21. J. Coutures, M. Foex, "Etude a haute temperature du diagrama d' equilibrie du systeme forme par le sesquioxyde d'yttrium", *J. Solid State Chem*., **11** (1974) 294–300.
22. G.C. Wei, T. Emma, W.H. Rhodes, S. Horvath, M. Harmer, "Analytical microscopy study of phases and fracture in Y_2O_3-La_2O_3 alloys", *J. Am. Ceram. Soc*., **71** (1988) 820–825.
23. W.H. Rhodes, "Controlled transient solid second phase sintering of yttria", *J. Am. Ceram. Soc*., **64** (1981) 13–17.
24. A.V. Shevchenko, B.S. Nigmanov, Z.A. Zaitseva, L.M. Lopato, "Interaction of samarium and gadolinium oxides with yttrium oxide" (in Russian), *Izv. Akad. Nauk. SSSR Neorg. Mater., 22 (1986) 775–*778.
25. M. Zinkevich, "Thermodynamics of rare earth sesquioxides", *Prog. Mater. Sci.*, **52** (2007) 597–647.
26. S.A. Toropov, *Phase Diagrams of the Refractory Oxide Systems, Binary systems* (in Russian), Nauka, Leningrad. 1987, pp. 822.
27. Y. Zhang, "Thermodynamic Properties of Rare Earth Sesquioxide", *M.Sc. thesis*, McGill University, Montreal, QC, Canada, 2016.
28. R. Horyń, E. Bukowska, A. Sikora, "Phase relations in La_2O_3-Gd_2O_3-CuO system at 950 °C", *J. Alloys Compd.*, **416** (2006) 209–213.
29. S.J. Schneider, R.S. Roth, "Phase equilibria in systems involving the rare-earth oxides. Part II. Solid state reactions in trivalent rare-earth oxide systems", *J. Res. Natl. Bur. Stand. A Phys. Chem*., **4** (1960) 317–332.
30. O.R. Andrievskaya, O.A. Kornienko, O.I. Bykov, "Interaction between lanthanum oxide and gadolinium at a temperature of 1100 °C", *Modern Problems of Physical Materials Science* (in Ukrainian), **26** (2017) 23–30.
31. O.R. Andrievskaya, O.A. Kornienko, O.I. Bykov, O.V. Chudinovich, L.N. Spasonova, "The interaction between cerium dioxide, lanthanum and europium oxides at 1500 °C", *Process. Appl. Ceram*., **15** (2021) 32–39.
32. L.G. Axelrud, Yu.N. Grin, P.Yu. Zavaliy, *Software Package for Structural Analysis of Crystals - CSD. General description*, Lviv, 1990.
33. O.V. Chudinovych, O.R. Andrievskaya, J.D. Bogatyryova, V.V. Kovylyaev, O.I. Bykov, "Phase equilibria in the La_2O_3-Y_2O_3-Nd_2O_3 system at 1500 °C", *J. Eur. Ceram. Soc*., **41** (2021) 6606–6616.
34. O.V. Chudinovych, O.R. Andrievskaya, J.D. Bogatyryova, O.I. Bykov, "Interaction of the lanthana, yttria with samaria at temperature 1500 °C" (in Ukrainian), *J. Chem. Technol*., **26** (2018) 20–30.
35. O.V. Chudinovych, O.I. Bykov, "Interaction of yttrium, lanthanum and erbium oxides at the temperature of 1500 °C" (in Ukrainian), *Vop. Khim. Khim. Tekhn.*, **4** (2020) 194–200.
36. O.V. Chudinovych, O.R. Andrievskaya, "Interaction of lanthanum, yttrium and ytterbium oxides at a temperature of 1500 °C" (in Ukrainian), *ONU Bulletin. Series: Chemistry*, **21** (2016) 53–66.